

## Supporting Information for

### Direct catalytic conversion of cellulose to liquid straight-chain alkanes

Beau Op de Beeck, Michiel Dusselier, Jan Geboers, Jensen Holsbeek, Eline Morr , Steffen Oswald, Lars Giebeler and Bert F. Sels

#### Table of contents

Table of contents .....	1
Experimental details: catalyst synthesis & characterization.....	2
Experimental section .....	2
Phase affinity .....	3
CO chemisorption.....	3
Scanning electron microscopy (SEM) + Energy-dispersive X-ray spectroscopy (EDS) .....	5
Inductively coupled plasma – atomic emission spectroscopy (ICP-AES) .....	6
Fourier transform infrared (FTIR) spectroscopy .....	6
X-ray powder diffraction (XRD).....	7
Experimental details: reaction analysis .....	8
Experimental section .....	8
High performance liquid chromatography (HPLC) .....	10
Gas phase analysis.....	11
References .....	13

## Experimental details: catalyst synthesis & characterization

### Experimental section

For htTSA(x)Ru/C synthesis, commercial 5 wt.% Ru/C (1 g, Sigma-Aldrich), tungstosilicic acid (TSA) hydrate (leading to x mM aqueous TSA concentration, Table S1, Sigma-Aldrich) and distilled water (40 ml) were loaded in a 100 ml stainless steel reactor (Parr Instruments Co.). The volume of the aqueous solution after complete TSA dissolution was measured and used in TSA concentration calculations. The reactor was first flushed with N<sub>2</sub> and subsequently pressurized with 5 MPa H<sub>2</sub>. The mixture was stirred at 700 rpm and heated to 483 K at an average rate of 10 K min<sup>-1</sup> and kept at this temperature for 1 h. After pretreatment, the reactor was cooled, depressurized and opened. The synthesized catalyst was filtered, thoroughly washed with distilled water and dried to constant weight (Table S1). No significant loss was observed during catalyst transfer from reactor to filter. However, minor catalyst loss (<8 wt.%) was observed after recuperation of catalysts from the filter. In reactions with cellulose and intermediates, 50; 25 or 12.5 wt.% of the recuperated amount was added (except for htRu/C: 0.5 g was added). A <8 wt.% deviation in added Ru/C is not expected to cause significant differences in product yield. In glucose/HMF hydrogenation reactions 25 wt.% of the filtered amount was added. Catalyst water content was determined at 473 K (full dehydration of TSA was observed at this temperature) by thermogravimetric analysis with a TGA Q500 from TA Instruments.

Leaching of Ru during htTSA(135)Ru/C synthesis was estimated with ICP-AES. After filtration over a 0.45 μm PES filter, Ru content was measured with an ICP-AES instrument (Ultima, Jobin Yvon Emission Horiba Group). An negligible amount of 0.3 wt.% of the Ru content in 1 g Ru/C was found in the filtrate.

**Table S1.** htTSA(x)Ru/C synthesis.

Catalyst <sup>[a]</sup>	TSA hydrate [g]	Weight after filtration [g]
htTSA(135)Ru/C	20	1.40 ± 0.03 <sup>[b]</sup>
htTSA(71)Ru/C	10	1.34
htTSA(37)Ru/C	5	1.34
htTSA(15)Ru/C	2	1.28
htTSA(8)Ru/C	1	1.14
htTSA(2)Ru/C	0.25	1.08 ± 0.03 <sup>[c]</sup>
htRu/C	0	1.00

[a] ht, hydrothermal treatment; x, [TSA]. [b] Average and standard deviation of 8 syntheses. [c] Average and standard deviation of 12 syntheses.

## Phase affinity

Figure S1 represents Ru/C and htTSA(135)Ru/C suspended in water/*n*-decane biphasic medium. Both catalysts clearly show an affinity for the *n*-decane phase. This pronounced *n*-decane affinity is in all probability caused by the apolar nature of the carbon support.



**Figure S1.** Ru/C and htTSA(135)Ru/C suspended in water/*n*-decane biphasic medium.

## CO chemisorption

CO chemisorption was employed to monitor changes in Ru dispersion and accessibility induced by hydrothermal pretreatment and TSA adsorption for Ru/C, htRu/C, htTSA(2)Ru/C and htTSA(135)Ru/C. 30 mg of catalyst was loaded into a tubular reactor, pretreated in a stream of 10 ml/min of H<sub>2</sub> at 423 K (heating rate: 5 K min<sup>-1</sup>) for one hour to reduce any present Ru<sup>4+</sup> to Ru<sup>0</sup> and subsequently cooled to room temperature in He (Air Liquide, 99.9997%). For the titration of the Ru surface, the He flow was set at 10 ml/min and pulses of 5 ml 100% CO (Air Liquide, 99.97%) were given with an interval of 2 minutes. The CO concentration in the outlet stream was followed with a Pfeiffer Omnistar quadrupole mass spectrometer. Table S2 presents the amount of moles CO adsorbed per mole of Ru and Ru dispersion, the latter calculated in the assumption that one CO molecule adsorbs per accessible Ru atom. Ru dispersion was only calculated for Ru/C and htRu/C due to possible TSA interference in CO chemisorption. A decrease in accessible Ru sites was observed upon modification and this decrease is linearly correlated with the initial glucose hydrogenation activity of the different catalysts (Figure S2). On the contrary, the initial HMF hydrogenation activity of the different catalysts appears to be more or less inversely correlated to the number of accessible sites. **Table S2.** Ru accessibility and dispersion for every catalyst.

Catalyst	mol CO adsorbed/mol Ru	Ru dispersion
Ru/C	0.46	46
htRu/C	0.38	38
htTSA(2)Ru/C	0.27	/
htTSA(135)Ru/C	0.12	/

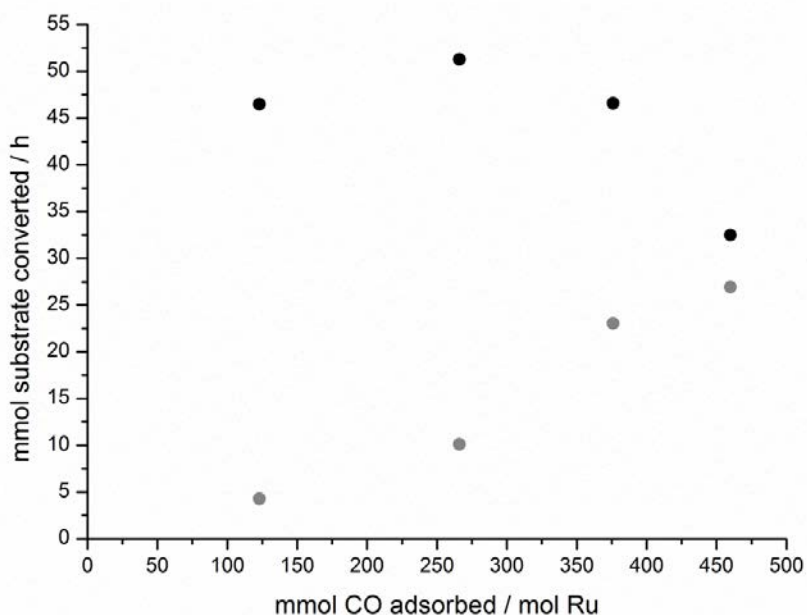


**Figure S2a.** Initial glucose (grey) and HMF (black) hydrogenation activity as a function of Ru accessibility. Reaction conditions: 5.56 mmol substrate, 0.25 g Ru/C (content in the different catalysts), 50 ml H<sub>2</sub>O, 5 MPa H<sub>2</sub>, 373 K (glucose) or 333 K (HMF).

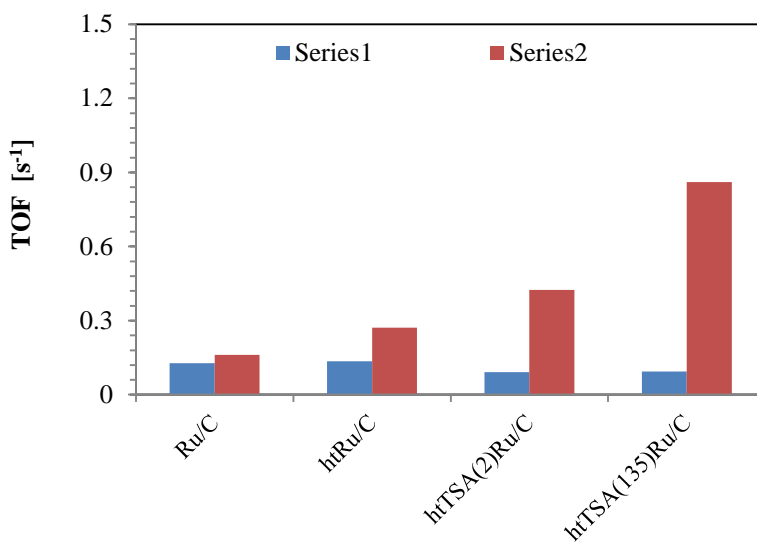


**Figure S2b.** Turnover frequency (calculated as mol converted substrate per mol surface Ru atoms per seconds). The data of Figure S2a and the chemisorption data in Table S2 at page 3 were used. Series 1 present TOFs in case of glucose, while series 2 are TOFs in case of reactions with HMF.

## Scanning electron microscopy (SEM) + Energy-dispersive X-ray spectroscopy (EDS)

SEM and EDS characterization was performed on Ru/C, htRu/C, htTSA(2)Ru/C and htTSA(135)Ru/C using a high resolution SEM (Philips XL-30 FEG), equipped with an EDS detector system from EDAX. Samples were sputtered with carbon before measurement. The length of the black bar in SEM micrographs represents 5  $\mu\text{m}$ . Due to the decrease in Ru dispersion caused by hydrothermal pretreatment, relatively more Ru is measured for htRu/C compared to Ru/C. The amount of adsorbed TSA for catalyst surfaces visualized with SEM was estimated based on the W/Ru wt.% ratio after quantitative EDS analysis and compared with gravimetric analysis (Table S3). Although these estimations match well for htTSA(2)Ru/C, a discrepancy is observed for htTSA(135)Ru/C: this could be due to the limited accuracy of the quantification methods or the less uniform distribution of TSA on the Ru/C surface at high loadings.

**Table S3.** Estimation of adsorbed TSA (g dry weight).

Catalyst	Gravimetric analysis	EDS analysis
htTSA(2)Ru/C	0.047	0.049
htTSA(135)Ru/C	0.340	0.289

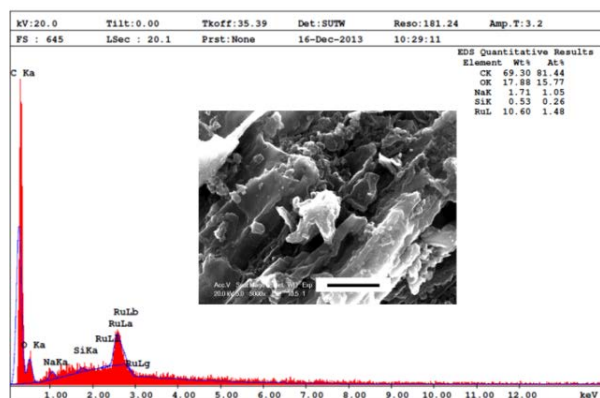


**Figure S3.** Ru/C

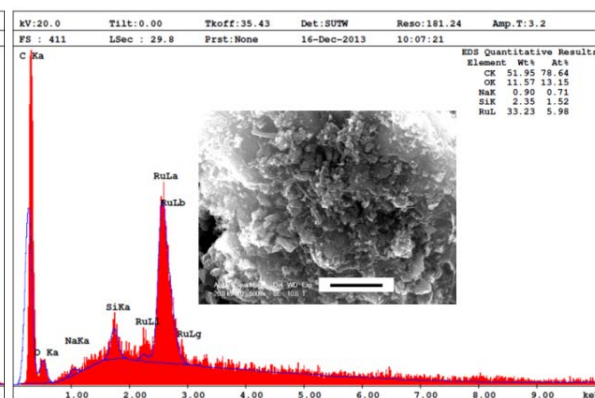


**Figure S4.** htRu/C

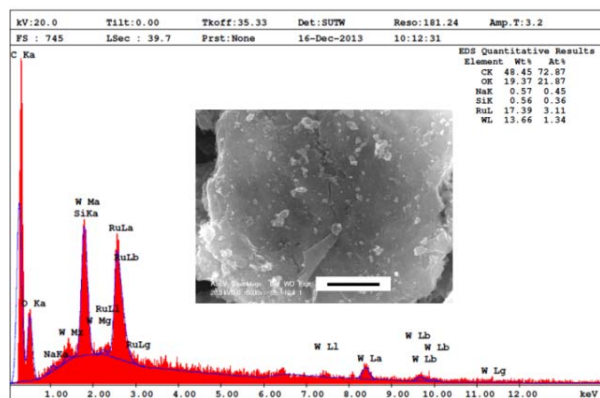


**Figure S5.** htTSA(2)Ru/C

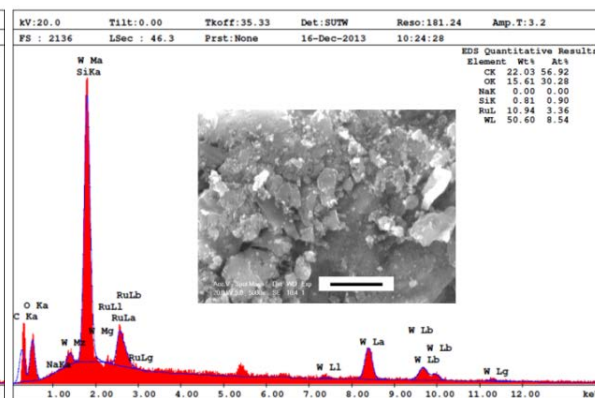


**Figure S6.** htTSA(135)Ru/C

## Inductively coupled plasma – atomic emission spectroscopy (ICP-AES)

ICP-AES was applied to estimate the amount of TSA adsorbed in htTSA(135)Ru/C (Table S4). After burning the htTSA(135)Ru/C catalyst in a muffle furnace at 1273 K for 15 min., the residue was dissolved in 0.42N HNO<sub>3</sub> and tungsten content was measured with an ICP-AES instrument (Ultima, Horiba Jobin Yvon). TSA content was calculated according to the measured tungsten content. However, a large discrepancy was observed between the gravimetric and ICP-AES determination.

**Table S4.** Estimation of adsorbed TSA (g dry weight).

Catalyst	Gravimetric analysis	ICP-AES analysis
htTSA(135)Ru/C	0.370	0.214

## Fourier transform infrared (FTIR) spectroscopy

FTIR spectroscopy was performed under vacuum on a Bruker IFS 66v/S instrument (KBr method) (Figure S7). All catalysts, including TSA, were calcined at 638 K (80 K under the reported decomposition temperature of TSA)<sup>1</sup> for 20 h before measurement to reduce the carbon content and increase the TSA concentration as reported by Pizzio et al.<sup>2</sup> TSA-specific adsorption bands were observed: stretching vibrations  $\nu_2$ Si-O<sub>a</sub> (1020 cm<sup>-1</sup>),  $\nu$ W-O<sub>d</sub>/W=O<sub>d</sub> (982 cm<sup>-1</sup>),  $\nu_1$ Si-O<sub>a</sub> (928 cm<sup>-1</sup>),  $\nu$ W-O<sub>b</sub>/W-O<sub>b</sub>-W (883 cm<sup>-1</sup>),  $\nu_2$ W-O<sub>c</sub>/W-O<sub>c</sub>-W (785 cm<sup>-1</sup>),  $\nu_1$ W-O<sub>c</sub> (540 cm<sup>-1</sup>) and bending vibration  $\delta$ Si-O<sub>a</sub>/O<sub>a</sub>-Si-O<sub>a</sub> (476 cm<sup>-1</sup>).<sup>2-6</sup> Small shifts in vibration wavenumbers between bulk and adsorbed TSA could be due to polyoxometalate - support or interpolyoxometalate interactions.<sup>7</sup>

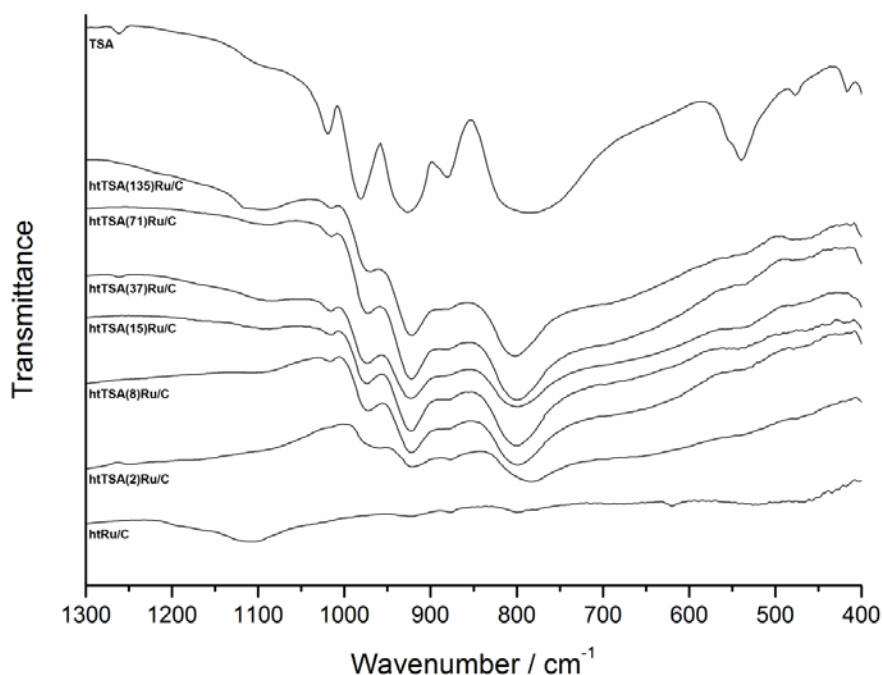


**Figure S7.** FTIR spectra of calcined catalysts.

## X-ray powder diffraction (XRD)

Crystallinity of all calcined catalysts, including TSA, was checked by XRD, recorded at room temperature on a STOE STADI P Combi diffractometer equipped with an image plate-position sensitive detector (IP-PSD). The diffracted intensity of Cu-  $K_{\alpha 1}$  radiation ( $\lambda = 0.15406$  nm) was measured in a  $2\theta$  range between  $0^\circ$  and  $62.2^\circ$ . Figure S8 presents XRD patterns of the calcined catalysts. The XRD pattern of calcined TSA corresponds well with the [00-001-0559] TSA\*6H<sub>2</sub>O database reference<sup>8</sup>, with intact TSA Keggin anions yielding characteristic reflections at  $2\theta = 17.9^\circ, 20.6^\circ, 25.2^\circ, 29.2^\circ, 34.5^\circ, 37.7^\circ$  and  $52.9^\circ$ . XRD analysis of calcined catalysts with low loadings revealed distinct reflections around  $2\theta = 28^\circ, 35^\circ, 40.2^\circ, 54.2^\circ, 57.9^\circ$  and  $59.4^\circ$ , which could be assigned to RuO<sub>2</sub> ([00-040-1290] RuO<sub>2</sub> database reference, space group  $P4_2/mnm$ )<sup>9</sup>. A graphite reflection can be observed around  $2\theta = 26.6^\circ$  ([00-056-0159] graphite database reference)<sup>10</sup>. However, XRD analysis of catalysts with higher loadings revealed distinct reflections around  $2\theta = 27.2^\circ, 36^\circ, 38.8^\circ, 53.9^\circ$  and  $56^\circ$ , which could not be directly linked to TSA. Indeed, several authors negate the formation of a crystalline phase upon impregnation of heteropoly acids on active carbon.<sup>2, 11</sup> Closer examination of the pattern revealed the presence of a second RuO<sub>2</sub> phase (space group  $P4_2/mnm$ ).<sup>12</sup> The transition of the RuO<sub>2</sub> phase might be caused by a TSA doping effect. The  $c/a$  ratio of the pristine tetragonal RuO<sub>2</sub> structure is changed significantly, *viz.*  $a$  becomes larger and  $c$  smaller. This transition appears to proceed stepwise with increasing TSA content.

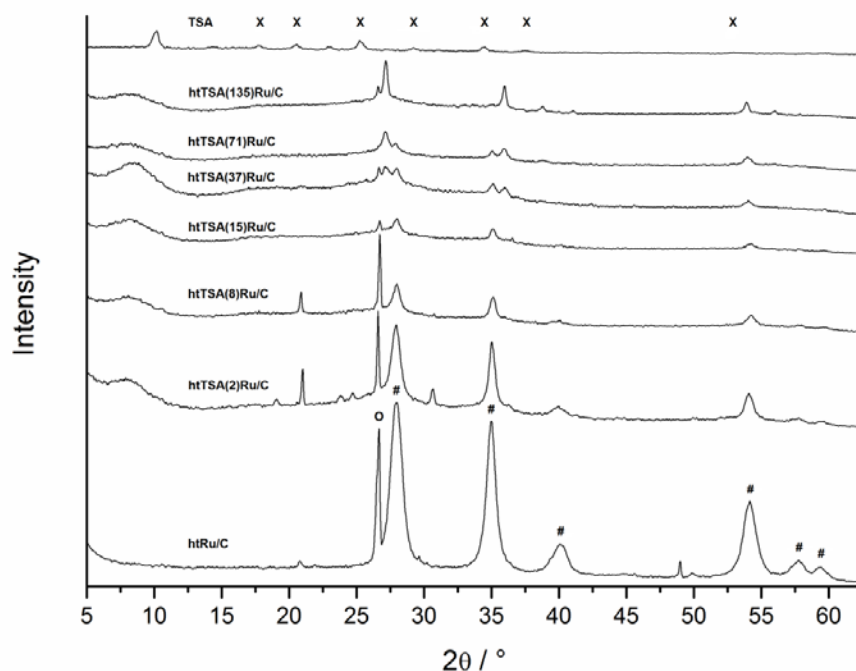


**Figure S8.** XRD patterns of calcined catalysts. XRD database reference reflections are indicated with symbols: TSA [00-001-0559] (X), RuO<sub>2</sub> [00-040-1290] (#) and graphite [00-056-0159] (O).

## Experimental details: reaction analysis

### Experimental section

Microcrystalline Avicel PH-101 cellulose, isosorbide, D-fructose, 5-hydroxymethylfurfural, 2,5-dimethyltetrahydrofuran, 2,5-hexanediol, 2,5-hexanedione, 1,2-hexanediol, TSA hydrate, 5 wt.% Ru/C and *n*-decane were purchased from Sigma-Aldrich. D-sorbitol was purchased from Janssen Chimica, D-glucose from Fischer Chemical and 1- and 2-hexanol from Acros Organics. Softwood sawdust was obtained from a local sawmill and sieved to a fraction between 250-500  $\mu\text{m}$ . Softwood, cellulose, TSA hydrate and Ru/C water content was determined by thermogravimetric analysis with a TGA Q500 from TA Instruments.

The sugar composition of softwood was determined using a combination of a reported standard procedure for total sugar determination with reported hydrolysis conditions for cellulose-rich materials.<sup>13, 14</sup> The formed alditol acetates were separated by using a Supelco SP-2380 polar column (30 m \* 0.32 mm i.d.; 0.2  $\mu\text{m}$  film thickness, Supelco, Bellefonte, PA, USA) in an Agilent 6890 series chromatograph (Agilent, Wilmington, DE, USA) equipped with autosampler, splitter injection port (split ratio 1:20), and flame ionization detector (FID). The carrier gas was He. Separation occurred at 498 K, injection and detection occurred at 543 K. The weight percentage of the sugar polymers was calculated from the weight percentage of the constituting sugars using a correction factor for hydrolysis water (0.9 for polyhexoses and 0.88 for polypentoses). Total polysaccharide content was estimated to be 64.2%, consisting of 57.7% polyhexose and 6.5% polypentose.

In a typical monophasic hydrogenation experiment, glucose (1 g), Ru/C (0.25 g) and water (50 ml) were loaded in a 100 ml stainless steel batch reactor. The reactor was first flushed with  $\text{N}_2$ . The reactor was stirred at 700 rpm and heated to 373 K. The reactor was then pressurized with 5 MPa  $\text{H}_2$ . This moment was chosen as the reaction starting time. At regular time intervals, samples were taken from the reaction solution. Samples were quickly cooled and centrifuged before GC and HPLC analysis.

In a typical biphasic batch experiment, microcrystalline Avicel PH-101 cellulose (2 g), TSA hydrate (5 g), htTSA(2)Ru/C (0.5 g), water (20 ml) and *n*-decane (20 ml) were loaded in a 100 ml stainless steel batch reactor (Parr Instruments Co.). The reactor was first flushed with  $\text{N}_2$  and subsequently pressurized with 5 MPa  $\text{H}_2$ . The mixture was stirred at 700 rpm and heated to 493 K at an average heating rate of 12 K  $\text{min}^{-1}$  from room temperature to 423 K and at a fixed rate of 0.5 K  $\text{min}^{-1}$  from 423 K to 493 K. The mixture was kept at 493 K for an additional 40 min. After reaction, the reactor was cooled, depressurized and opened. For yield-temperature/time plots, the reactor was rapidly cooled after the respective temperature/time was reached. For gas analysis, the reactor was depressurized into a gas cylinder of which the content was analyzed by GC. Samples were taken from both water and *n*-decane phases and centrifuged before GC, HPLC and TOC analysis. For conversion determination, centrifuged particles were resuspended, added back to the reaction mixture and filtered with the rest of the solid particles in the reaction mixture. The solid residu was thoroughly washed with water and acetone and dried to constant weight. Any solid humin fraction formed can partially dissolve in acetone.<sup>15</sup>

In a typical biphasic fed-batch experiment, a 100 ml stainless steel fed-batch reactor was loaded with 0.5 g htTSA(2)Ru/C and 20 ml *n*-decane. The reactor was first flushed with  $\text{N}_2$  and subsequently pressurized with 5 MPa  $\text{H}_2$ . The mixture was stirred at 750 rpm. The aforementioned temperature-time program for

batch reactions was also used here. After reaching 423 K, 20 ml of an aqueous solution containing feedstock, TSA and water (concentrations comparable to the reference batch reaction) was fed gradually into the reactor at a constant flow rate of 0.111 ml min<sup>-1</sup> with a Waters 515 HPLC pump until the end of the reaction. After reaction, the reactor was cooled and samples were taken and analyzed in the same way as in the batch experiment.

GC analysis of both aqueous and *n*-decane samples was performed on a Hewlett Packard 5890 GC equipped with an HP 7673 autosampler, a 60 m HP-1 column, and a FID. Aqueous samples were derivatized to trimethylsilyl ethers before GC analysis. For product identification, GC-MS analysis of underivatized aqueous samples was performed on an Agilent 6890 Series GC equipped with a 30 m HP-5MS column (internal diameter 0.25 mm, film thickness 0.25 μm) and an Agilent 5973 Network MS, while GC-MS analysis of *n*-decane samples was performed on an Agilent 6890N Network GC system equipped with a 30 m HP-1MS Ultra Inert column (internal diameter 0.25 mm, film thickness 0.25 μm) and an Agilent 5973 Network MS. HPLC analysis of aqueous samples was performed on an Agilent 1200 Series HPLC equipped with a Varian Metacarb 67C column (300 \* 6.5 mm, mobile phase: water) and a RID, after neutralization of TSA with Cs<sub>2</sub>CO<sub>3</sub> and filtration over a 0.45 μm NY filter. The total amount of organic carbon (TOC) in aqueous samples was determined using an Analytik Jena Multi N/C 2100 TOC Analyzer equipped with an IR detector.

GC analysis of the gaseous phase was performed on an Interscience Trace GC equipped with Hayesep Q and RTX-1 columns and a FID and TCD.

Product yields are expressed as C mol%: yield (%) = (moles C in product / moles C in feedstock) \* 100. Softwood product yields were expressed as: yield (%) = (moles C in product / moles C in polysaccharides) \* 100. Product yields of other *n*-decane-soluble products besides *n*-hexane, methylcyclopentane, cyclohexane, *n*-pentane, 2,5-dimethyltetrahydrofuran and 1- or 2-hexanol were not estimated separately due to their low concentration, instead GC peak areas were summed and the C mol% yield was calculated in the same way as *n*-hexane. Product yields of other water-soluble products besides glucose and hexitols (and their anhydrides) were calculated based on the difference between TOC yield ((moles C in aqueous phase / moles C in feedstock) \* 100) and hexitol yield determined by GC. Cellulose conversion was determined gravimetrically: conversion (%) = (initial cellulose weight - weight of the solid residu after reaction - initial catalyst weight) / (initial cellulose weight) \* 100. The difference between conversion and total dissolved product yield was assigned as insoluble product yield. The volume of the aqueous solution after complete TSA dissolution was measured and used in TSA concentration and yield calculations.

Cracking of *n*-decane to lower alkanes was investigated in a blank reaction without cellulose (manuscript Table 2, entry 2 conditions, htTSA(71)Ru/C). Only minor amounts of *n*-decane cracking/isomerization products were observed: mainly heptane and a negligible amount of *n*-hexane (3.5 mg, which would amount to <1% yield based on cellulose). Heptane was rarely observed in product mixtures, suggesting that cracking of *n*-decane probably only occurs in substrate-deficient reactions.

Leaching of TSA into the aqueous phase was estimated with ICP-AES for a reaction without TSA hydrate added to the reaction mixture (manuscript Table 1, entry 6, htTSA(135)Ru/C). After filtration over a 0.45 μm NY filter, an aqueous sample was diluted in 0,42N HNO<sub>3</sub> and tungsten content was measured with an ICP-AES instrument (Ultima, Horiba Jobin Yvon). TSA content was calculated according to the measured

tungsten content. An estimated amount of 22% of the TSA content of htTSA(135)Ru/C was found in the aqueous phase.

In htTSA(15)Ru/C recycling experiments, samples were taken from both aqueous and *n*-decane phases after reaction and centrifuged before GC and TOC analysis. Centrifuged catalyst particles were resuspended, added back to the reaction mixture and filtered with the rest of the catalyst particles in the reaction mixture. The catalyst residue was thoroughly washed, dried to constant weight and reused in a subsequent experiment.

In htTSA(2)Ru/C recycling experiments, samples were taken from both aqueous and *n*-decane phases after reaction and centrifuged. 500  $\mu$ l supernatant of both phase samples was used for GC analysis. Subsequently, samples were replenished with 500  $\mu$ l water or *n*-decane. Centrifuged catalyst particles were resuspended after which both phase samples were fully re-administered to the reaction mixture. After addition of fresh cellulose, a new experiment was started.

### High performance liquid chromatography (HPLC)

Figure S9 presents the HPLC chromatograms of the aqueous phase during the conversion of microcrystalline cellulose to liquid alkanes with TSA and htTSA(2)Ru/C in function of time and temperature in manuscript Table 4, entry 4 conditions. The assigned products were identified with corresponding reference compounds.

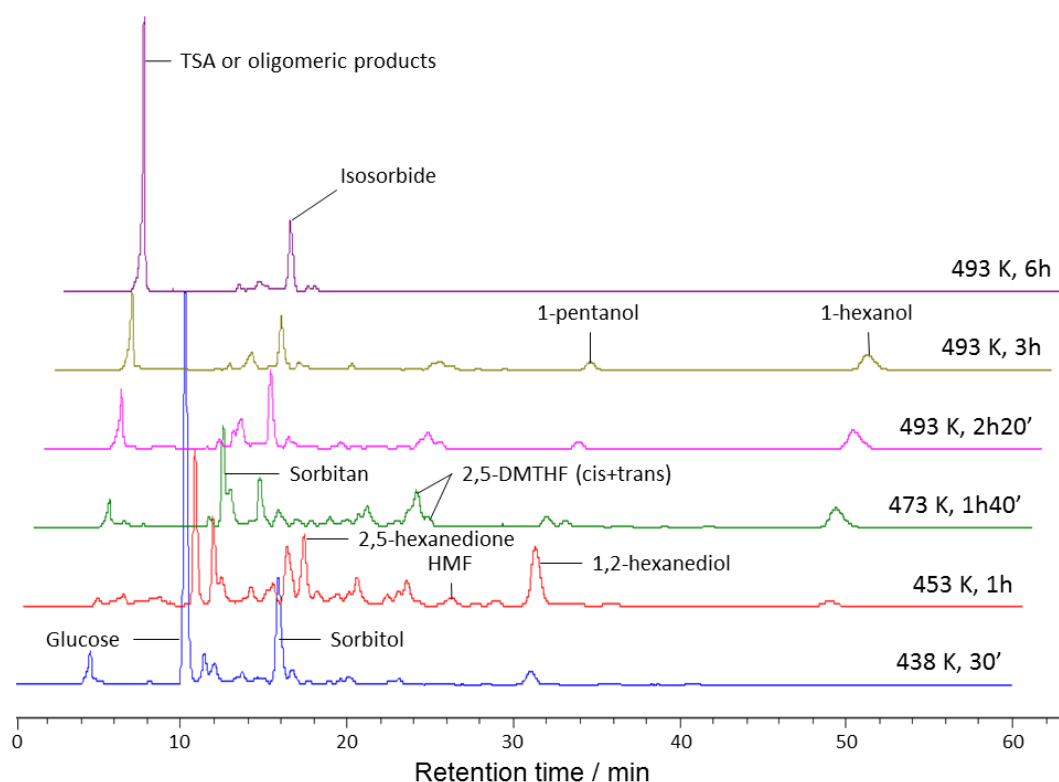


**Figure S9.** HPLC chromatograms of the aqueous phase during the conversion of microcrystalline cellulose to liquid alkanes with TSA and htTSA(2)Ru/C in function of time and temperature. Reaction conditions: manuscript Table 4, entry 4.

## Gas phase analysis

Figures S10 and S11 present the GC-FID and GC-TCD chromatograms, respectively, of the headspace gas of a typical cellulose reaction. Figures S12 and S13 present the GC-FID and GC-TCD chromatograms, respectively, of the headspace gas of the 1-hexanol reaction (manuscript Table 3, entry 18). Identified gaseous alkanes were assigned.

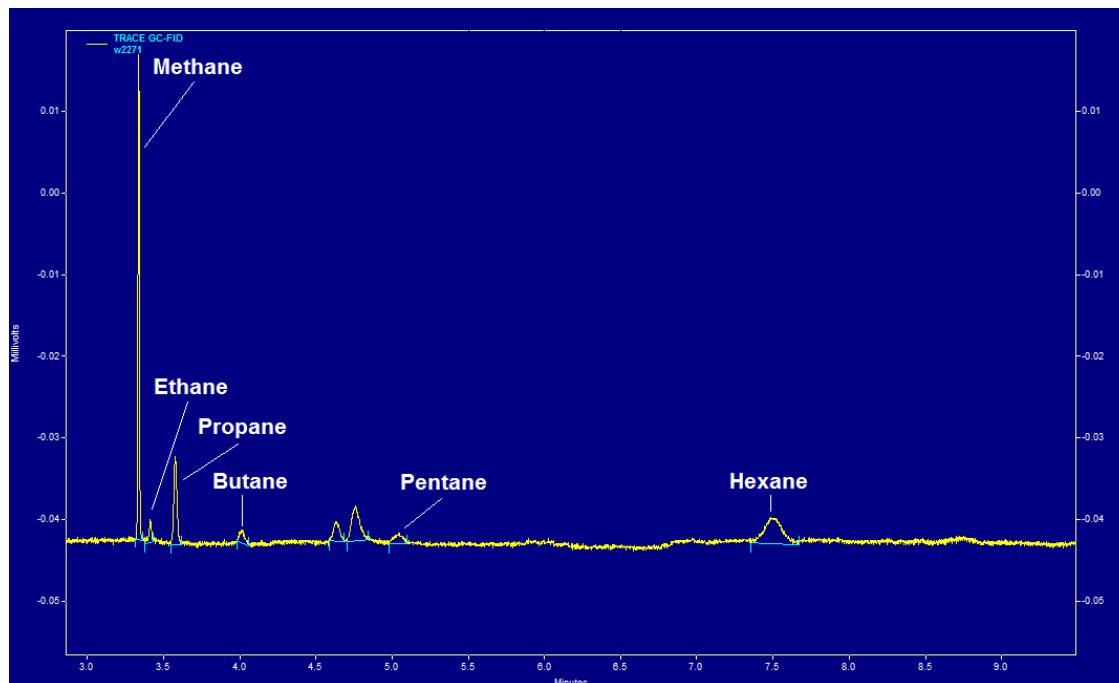


*Figure S10.* GC-FID chromatogram of a typical cellulose reaction.

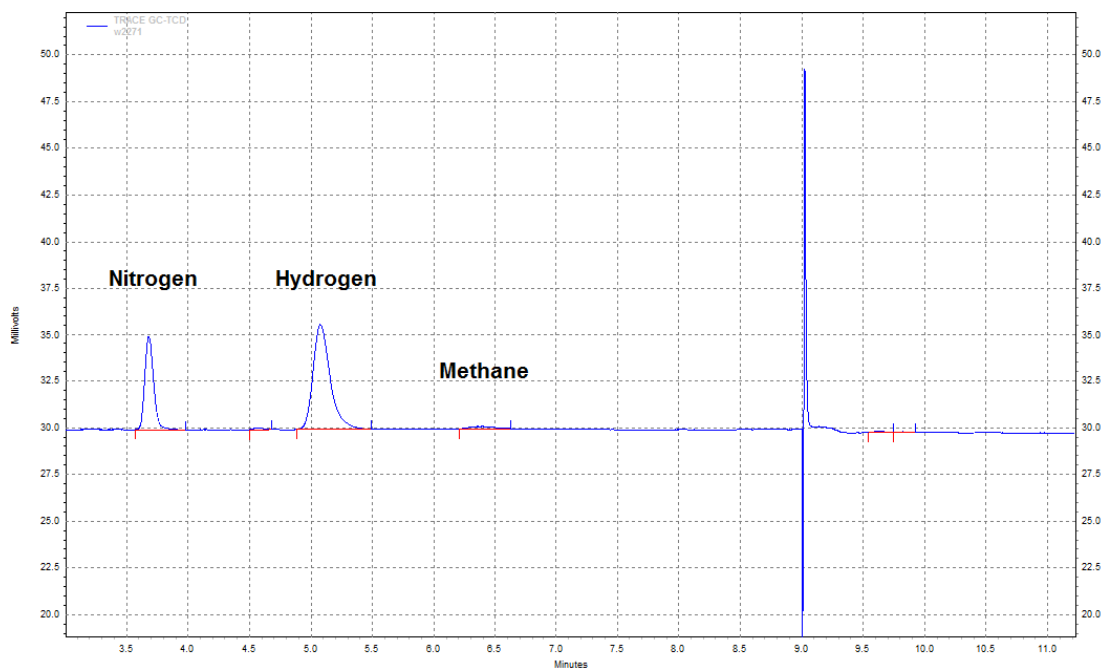


*Figure S11.* GC-TCD chromatogram of a typical cellulose reaction.

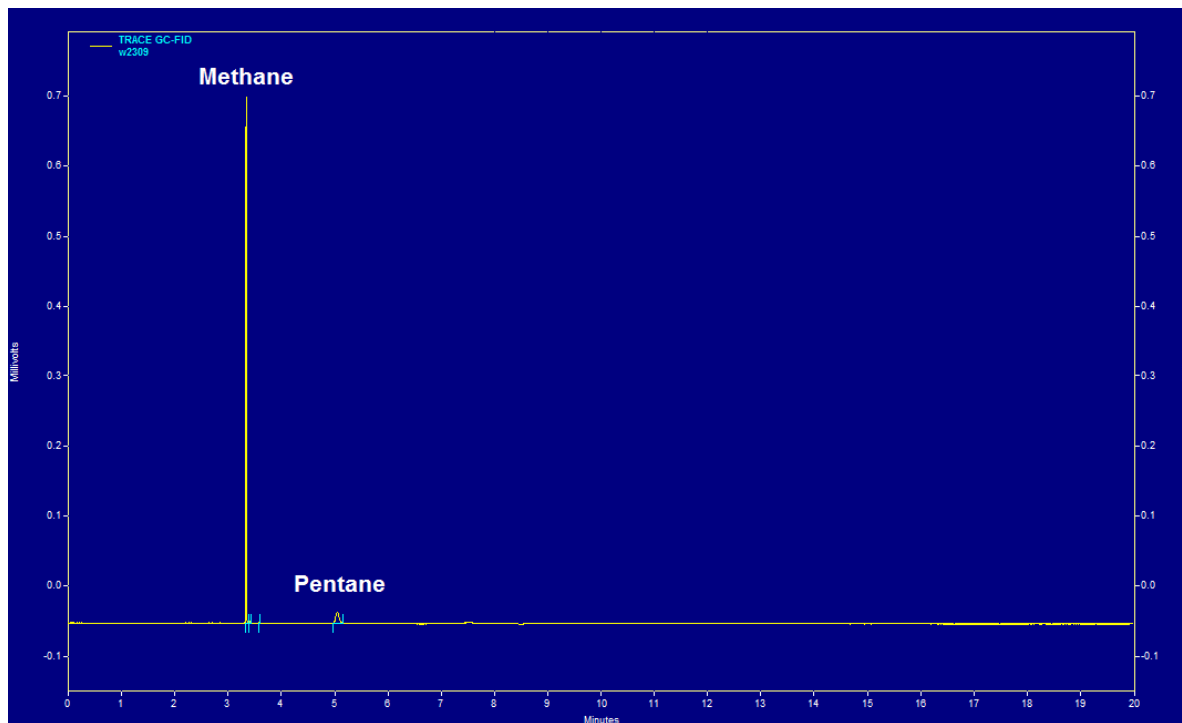


Figure S12. GC-FID chromatogram of the 1-hexanol reaction.

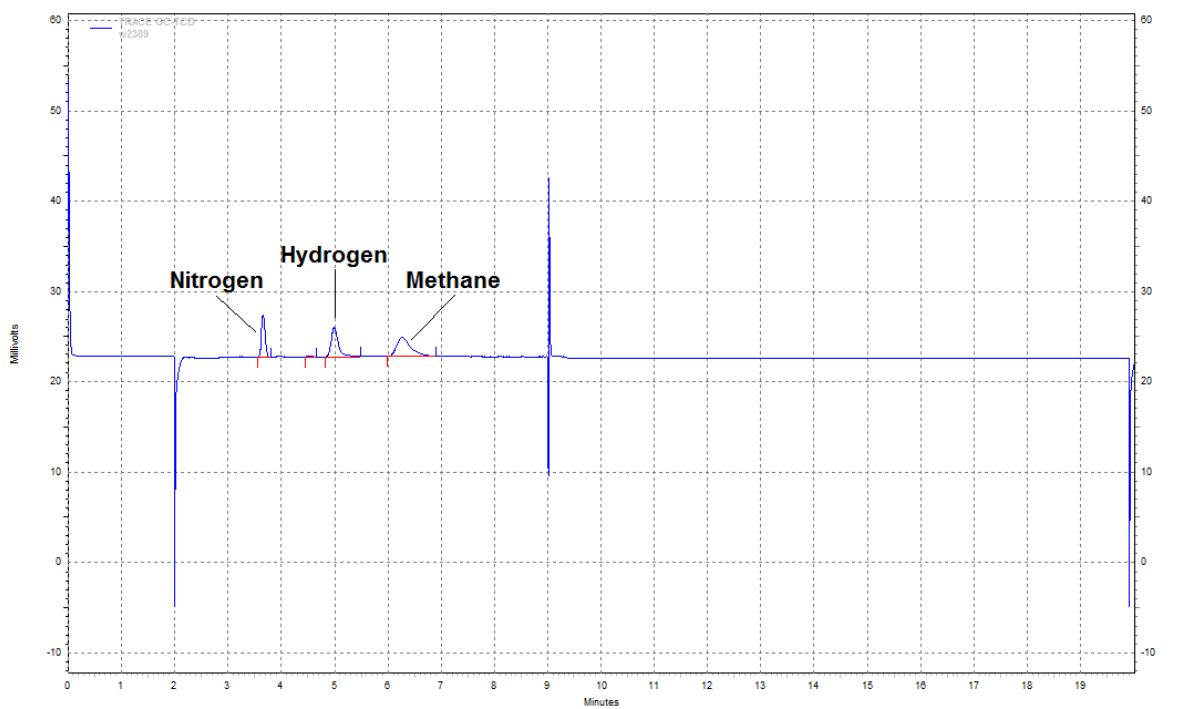


Figure S13. GC-TCD chromatogram of the 1-hexanol reaction.

## References

1. V. F. Chuvaev, K. I. Popov and V. I. Spitsyn, *Dokl. Akad. Nauk. SSSR*, 1980, **255**, 892.
2. L. R. Pizzio, C. V. Cáceres and M. N. Blanco, *J. Col. Interf. Sci.*, 1997, **190**, 318-326.
3. M. Klisch, *J. Sol-Gel Sci. Technol.*, 1998, **12**, 21-33.
4. T. Okuhara, N. Mizuno and M. Misono, *Adv. Catal.*, 1996, **41**, 113-252.
5. C. Rocchiccioli-Deltcheff, R. Thouvenot and R. Franck, *Spectrochim. Acta A*, 1976, **32**, 587-597.
6. R. Thouvenot, M. Fournier, R. Franck and C. Rocchiccioli-Deltcheff, *Inorg. Chem.*, 1984, **23**, 598-605.
7. J.-P. Tessonier, S. Goubert-Renaudin, S. Alia, Y. Yan and M. A. Barteau, *Langmuir*, 2012, **29**, 393-402.
8. A. G. Scroggie and G. L. Clark, *Proc. Natl. Acad. Sci. U. S. A.*, 1929, **15**, 1-8.
9. C. E. Boman, *Acta Chem. Scand.*, 1970, **24**, 116-122.
10. J. Y. Howe, C. J. Rawn, L. E. Jones and H. Ow, *Powder Diffr.*, 2003, **18**, 150-154.
11. I. V. Kozhevnikov, A. Sinnema, R. J. J. Jansen and H. Bekkum, *Catal. Lett.*, 1994, **27**, 187-197.
12. M. L. Foo, Q. Huang, J. W. Lynn, W.-L. Lee, T. Klimczuk, I. S. Hagemann, N. P. Ong and R. J. Cava, *J. Solid State Chem.*, 2006, **179**, 563-572.
13. C. M. Courtin, H. Van den Broeck and J. A. Delcour, *J. Chromatogr. A*, 2000, **866**, 97-104.
14. C. Gourson, R. Benhaddou, R. Granet, P. Krausz, B. Verneuil, P. Branland, G. Chauvelon, J. F. Thibault and L. Saulnier, *J. Appl. Polym. Sci.*, 1999, **74**, 3040-3045.
15. I. V. Sumerskii, S. M. Krutov and M. Y. Zarubin, *Russ. J. Appl. Chem.*, 2010, **83**, 320-327.